

Grease-lubricated tribological contacts – Influence of graphite, graphene oxide and reduced graphene oxide as lubricating additives in lithium complex (LiX)- and polypropylene (PP)-thickened greases

Elin Larsson ^{a,*}, René Westbroek ^b, Johan Leckner ^b, Staffan Jacobson ^a, Åsa Kassman Rudolphi ^a

^a Ångström Tribomaterials Group, Uppsala University, Box 35, 751 03, Uppsala, Sweden

^b Axel Christiernsson International AB, Nol, Sweden

ARTICLE INFO

Keywords:

Grease
Friction
Additive
Graphene oxide
Electrical contacts
4-ball tests

ABSTRACT

Two types of thickener systems, lithium complex (LiX) and polypropylene (PP), were chosen to evaluate graphite, graphene oxide (GO) and reduced graphene oxide (rGO) as grease additives at a concentration of 0.1 wt %. To enhance the additive dispersibility, a mixture of polyalphaolefin oil (PAO) and oil soluble synthetic polyalkylene glycol (OSP-68) was used as base oil. The greases were evaluated in i) silver-coated copper contacts simulating high-load electrical contact applications subjected to fretting and ii) a steel/steel 4-ball wear test equipment. The additives showed no positive effect on friction and wear, neither in fretting nor in 4-ball tests. However, there is a statistically significant difference in wear scar diameter on the 4-ball steel contacts between the two thickener types, LiX and PP. Thus, the PP-grease lubricated steel contacts showed more wear and more tribofilms of iron oxide and grease constituents, indicating more metal-to-metal contact. Hence, the thickener type has a larger impact on the lubricating performance of the grease than do the graphite, GO and rGO additions. The results demonstrate that the addition of graphene-based materials to improve greases is not straightforward. Rather, the grease/graphene-based additive system is complex and many parameters influence the friction and wear results. Hence, more work is needed to obtain a better understanding and possibly better lubricating effects from the graphene-based additives.

1. Introduction

Graphene and graphene-based materials have been widely investigated in various fields for their mechanical, chemical, electrical and tribological properties [1,2]. Graphene-based lubricants have become interesting for lubrication purposes of various applications, including electrical contacts. Graphene is a single atom-thick sheet of sp^2 -bonded carbon atoms [3], i.e., a single layer of graphite. The nomenclature or classification of graphene varies in the literature. For instance, Bianco et al. [3] proposed the following nomenclature in 2013: a 2D sheet-like material consisting of two to five well-defined stacked graphene layers is called few-layer graphene (FLG) and two to ten graphene layers is called multi-layer graphene (MLG). In the ISO standard of graphene and related two-dimensional materials from 2017 [4], a bilayer and trilayer of graphene is two and three well-defined stacked graphene layers, respectively, and few-layer graphene consists of three to ten well-defined stacked graphene layers. More than ten graphene layers

can be treated as bulk graphite since the electrical properties then are the same as for graphite. Despite this nomenclature, the term graphene is often used also for non-graphene carbon, sometimes even when the material according to definition is graphite.

Graphene has been reported to reduce friction and wear when used in oil [5–7], in greases [8–15] and when used as a solid lubricant [16–20]. Other graphene-based materials such as graphene oxide (GO) and reduced graphene oxide (rGO) have also been found to reduce friction and wear [10,21–25]. Among the literature references cited here, the contact geometry, contact load and contact material all vary, but nevertheless they all report positive effects of the additive. The study by Andersson [26] presents a more complex picture, where the addition of graphene and GO to grease does not always result in friction reductions. No conclusions regarding the lubricating effect could be drawn, neither regarding the influence from additive concentration (0.01, 0.05 and 0.1 wt%) nor from the additive type. This was due to large spread of friction results between test repetitions. The author states

* Corresponding author.

E-mail address: elin.larsson@angstrom.uu.se (E. Larsson).

that poor distribution and agglomeration of particles are possible reasons for the varying friction results and that a dispersion optimization probably is required.

GO is a single layer of graphite oxide with a high oxygen content [3, 27]. The structure of GO, i.e., the level of oxidation, varies with synthesis conditions [28]. rGO is a single layer of GO processed to reduce its oxygen content [3, 27]. A comparison of the chemical structures of graphene, GO and rGO is presented in Fig. 1. The oxygen functional groups in GO and rGO lower the electrical conductivity compared with graphene [29]. However, graphene is too expensive for many industrial applications, so alternatives that offer similar lubricating properties to a lower price are desirable. GO and rGO represent such possible alternatives, despite their inferior electrical conductivity. The price of graphene and GO varies with parameters such as purity and whether delivered as powder or as dispersion. If delivered as powder, the flake size and thickness will affect the pricing and if in dispersion the solvent and concentration, except from flake size and thickness, will. Worth to mention is that Kauling et al. [30], 2018 stated that the quality of graphene produced today is rather poor. The majority of 60 graphene producers investigated in their study are producing fine graphite instead of graphene. As part of overcoming this issue, a standard from 2021 [31], presents methods for characterizing the structural properties of graphene, bilayer graphene and graphene nanoplatelets from powders and liquid dispersions, including measurement protocols, sample preparation and data analysis. The standard includes number of layers/thickness of the flakes, the lateral flake size, the level of disorder, layer alignment and the specific surface area.

The present work aims at evaluating the potential of the graphene-based materials GO and rGO as additives in greases for friction and wear reduction in tribological contacts, and especially in electrical contact applications subjected to fretting. Graphite is used as a reference additive, and two base greases without any additives are used as reference baselines to the three greases with additive. The greases are evaluated with respect to fretting of electrical contacts, and in a 4-ball steel/steel wear test.

Electrical contacts should have a low and stable contact resistance, preferably below $50 \mu\Omega$ for high power applications. Further, non-stationary contacts should offer low coefficient of friction combined with high wear resistance, and must not form insulating films on the surfaces. The combination of low contact resistance, low coefficient of friction and high wear resistance is not easy to fulfill. Low contact resistance requires a large area of real contact, typically created by using soft contact materials (these soft materials are used as thin coatings on

harder substrates) and applying high contact loads, typically 10–100 N. The combination of copper substrate and silver coating is commonly used in many applications. In moving contacts with high applied loads, these coatings are expected to suffer large material deformation and wear. Various types of lubricants can be used to reduce the friction and wear. Today, most electrical contacts in high power applications are lubricated with oil or grease. Obviously, the lubricant must not completely separate the surfaces since metal-to-metal contact is required to maintain a low contact resistance.

1.1. Additives in grease

A grease is a semi-solid lubricant comprising a lubricating oil and a thickener, i.e., a grease is a thickened oil. The thickener may be a metal soap (lithium, aluminium, sodium, calcium, etc.), a metal complex soap (lithium complex, calcium complex, etc.) or a non-soap thickener (bentonite, silica-gel, polypropylene (PP), etc.). Further, the grease may include several additives, with different properties and functions. Examples include viscosity and rheology modifiers, oxidation and rust inhibitors, extreme pressure, anti-wear and friction reducing additives. The additives should preferably be easy to disperse in the grease matrix and should not impair the grease structure or properties. Polar additives are difficult to dissolve in a non-polar media, such as the base oil polyalphaolefin (PAO), and vice versa. However, the additives can be chemically modified to increase their solubility [5, 7, 32, 33]. Since the grease consistency itself prevents sedimentation, good solubility is less critical in greases than in oils [34].

For the tribological efficiency of additives that operate on surfaces, it is essential to reach and sometimes react with the metal surfaces. This is not important for additives that modify the viscosity and rheology, etc. The most polar species in the grease matrix are most likely to reach the sites on the metal surfaces [35]. For soap-thickened greases, the thickener will mostly win this race, due to its higher polarity. This means that the additives, most of which are highly polar [36], have to compete with the thickener. The best strategy for helping the additives to reach the surfaces is generally to have them dispersed in a grease with a non-polar thickener, such as PP. Note that a non-polar thickener may not always be better for the additive response (i.e., the ability of an additive to reduce friction and/or wear etc.), it all depends on the grease constituents. All in all, it can be concluded that adding additives and producing a well working grease is rather complex.

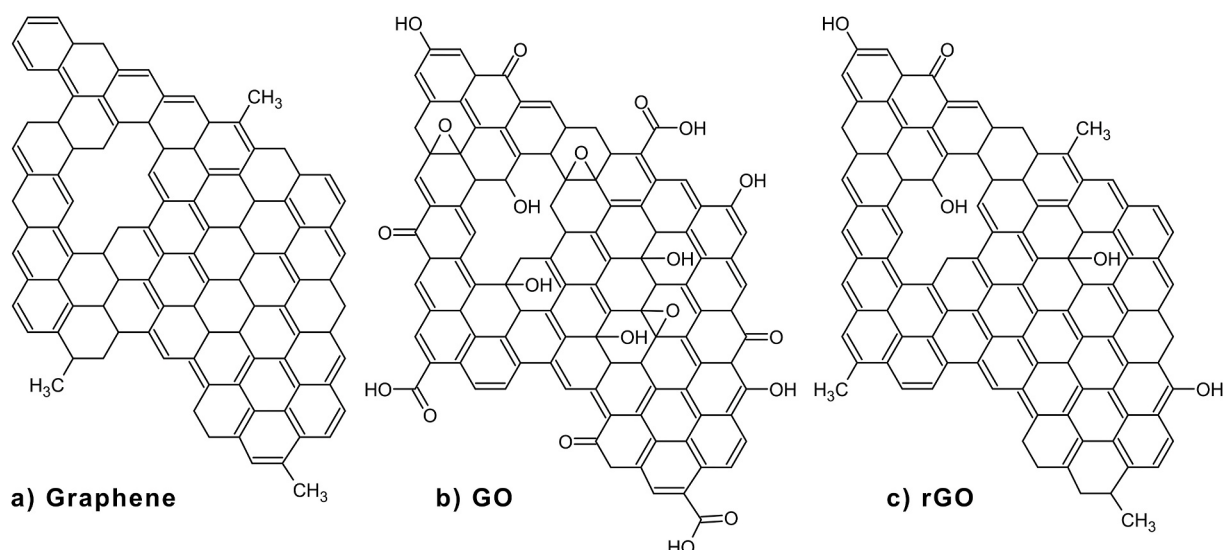


Fig. 1. Comparison of chemical structures of a) graphene, b) GO and c) rGO. Chemical structures from Ref. [28].

2. Materials and methods

2.1. Grease manufacturing

In the literature, graphene-based materials have sometimes been evaluated by addition to commercially available greases rather than in greases produced specifically for the study. The greases are then either heated and mixed [10,24] with an additive/solvent blend or just mixed with the additive [9,12–14]. In Ref. [15] the additives and commercial grease were dissolved in separate solvents before mixing the additives into the grease in various concentrations. In the present work, the greases are specially designed when it comes to the selection of thickener systems and oil types.

Two types of thickener systems, lithium complex (LiX) and PP, were chosen to evaluate graphite, GO and rGO as grease additives. LiX was chosen since it is by far the most common thickener type and PP was chosen since it is a non-polar thickener with many beneficial properties in comparison with LiX grease. Examples of such properties include longer grease life, better low temperature performance, lower friction and enhanced additive response (due to the non-polar thickener) [35,37,38]. The two selected thickener systems were also studied in previous work on grease-lubricated fretting of electrical contacts [39], but then without additives. The lubricating properties of the two thickener systems varied with the fretting displacement amplitude. Further, Shu et al. [40] studied the tribological performance of zinc dialkyldithiophosphate (ZDDP) and molybdenum dialkyldithiocarbamate (MoDTC) additives in LiX and PP greases.

A suitable oil is needed to disperse the GO and rGO additives in the grease matrix. In the previous study of grease-lubricated electrical contacts [39], an oil blend of 93.7 wt% PAO base oil (with kinematic viscosity of 10 cSt at 100 °C) and 6.3 wt% adipate ester was used. The low polarity of PAO results in poor dispersibility of polar additives such as GO and rGO. In nonpolar solvents, the dispersibility of rGO is typically somewhat better than that of GO, due to fewer oxygen-containing functional groups. To find the oil best suited for stable dispersion of GO and rGO, five different oils or oil blends were compared. The oils were: PAO, PAO/adipate ester as in Ref. [39], adipate ester, polyol ester and OSP-68 (Oil soluble synthetic polyalkylene glycol with kinematic viscosity of 68 cSt at 40 °C and 11.5 cSt at 100 °C). The scale of polarity, based on aniline point of the oils, from lowest to highest is: PAO < PAO/adipate ester < adipate ester ≈ polyol ester < OSP-68. OSP is a Group V base oil that can be used as a primary base oil, co-base oil and as a performance enhancing additive [41]. The OSP oil, which has a high polarity, can be used together with less polar oils to facilitate solvency of additives with a polar nature. rGO was most stable and easiest to disperse in the OSP-68 oil. Since the polarity is too high to prepare PP greases in 100% OSP-68, a mixture of 60 wt% PAO and 40 wt% OSP-68 was chosen for production of both LiX and PP greases. The dispersion of rGO in this oil blend was stable for more than 37 days. It should be mentioned that the solvent polarity, in this case the oil polarity, may not be the only factor influencing the additive's dispersibility [42].

LiX and PP greases based on the same oil blend as in Ref. [39] (PAO/adipate ester, hereafter only called PAO or PAO oil), were used as a reference to the PAO/OSP greases with and without additives. The evaluated greases are summarized in Table 1. The concentration of graphite, GO and rGO in the greases was 0.1 wt%. This concentration is the same as the optimized graphene concentration in grease found in Refs. [8,14]. The graphite, GO and rGO powders were used as received. Additive details are presented in Table 2. The graphite powder had a smaller particle size than both GO and rGO.

2.1.1. Manufacturing of LiX grease

A pilot reactor with a batch size of 8 kg was used to manufacture the LiX grease. The PAO/OSP oil blend and 12-hydroxystearic acid were mixed and heated to melt the fatty acid. After about an hour, LiOH and water were added. After this addition, the grease temperature was 85 °C.

Table 1

Evaluated greases.

Thickener	Oil blend	Additive	Name of the grease
PP	PAO/OSP ^a	–	PP PAO/OSP reference grease
		Graphite	PP PAO/OSP grease with graphite
		GO	PP PAO/OSP grease with GO
LiX	PAO/OSP ^a	rGO	PP PAO/OSP grease with rGO
		–	LiX PAO/OSP reference grease
		Graphite	LiX PAO/OSP grease with graphite
PP	PAO ^b	GO	LiX PAO/OSP grease with GO
		rGO	LiX PAO/OSP grease with rGO
		–	PP PAO reference grease
LiX	PAO ^b	–	LiX PAO reference grease

^a 60 wt% PAO-10 and 40 wt% OSP-68 (kinematic viscosity of 10 and 11.5 cSt at 100 °C, respectively).

^b 93.7 wt% PAO-10 (kinematic viscosity of 10 cSt at 100 °C) and 6.3 wt% adipate ester.

Table 2

Additive details according to the suppliers. For these distributions of particle sizes, 10% are smaller than the D10 diameter and 10% are larger than the D90 diameter.

Additive	Supplier	Particle size D10 [μm]	Particle size D90 [μm]
Graphite	Univar	2.18	8.70
GO	Graphenea	6.63	27
rGO	Graphenea	3–5	21–27

The temperature was then increased to remove the water from the grease mixture. After 2.5 h, azelaic acid was added followed by addition of LiOH and water. The temperature was increased once again to reach a grease temperature of 206 °C before starting to cool the grease by addition of small portions of oil. After cooling to room temperature, the grease was homogenized and deaerated for 1 h. The grease consistency was measured with cone penetration (NLGI consistency number 2) after homogenization and deaeration. The LiX PAO grease, as in Ref. [39], was manufactured in the same way as the LiX PAO/OSP grease. The LiX PAO grease is the same as was denoted LiX-10 in previous work [39].

2.1.2. Manufacturing of PP grease

The PP and the PAO/OSP oil blend were put in a round flask and heated in a mantle heater to melt the polymer. After complete melting, the oil/thickener mixture was quench-cooled below the melting temperature of PP. Three batches of 1200 g were prepared in the same way. The quenched material was mixed into the desired consistency in a mixing vessel, followed by a deaeration step. The consistency was measured during the mixing, as well as after deaeration (NLGI consistency number 2). The PP PAO grease, as in Ref. [39], was produced in the same way as for the PAO/OSP grease. The PP PAO grease is the same as was denoted PP-10 in previous work [39].

2.1.3. Addition of graphite, GO and rGO to LiX and PP greases

The three different additives were suspended in the PAO/OSP oil blend with an additive concentration of 5 wt%. An ultrasonic probe (QSONICA, Q55) was used at 50% amplitude setting four times 1 min, to suspend the additives in the oil blend. The additive/oil solutions were mixed with the LiX and PP PAO/OSP greases in a centrifugal mixer (SpeedMixer DAC 600) and the final additive concentration was 0.1 wt %. Images of all prepared greases are presented in Fig. 2. Graphite and GO were well dispersed in the greases. However, rGO was more difficult to disperse in the oil, resulting in visible black rGO particle agglomerates.

2.1.4. Thickener structure analysis

The LiX and PP thickener structures of the PAO and PAO/OSP reference greases, respectively, were investigated with a scanning

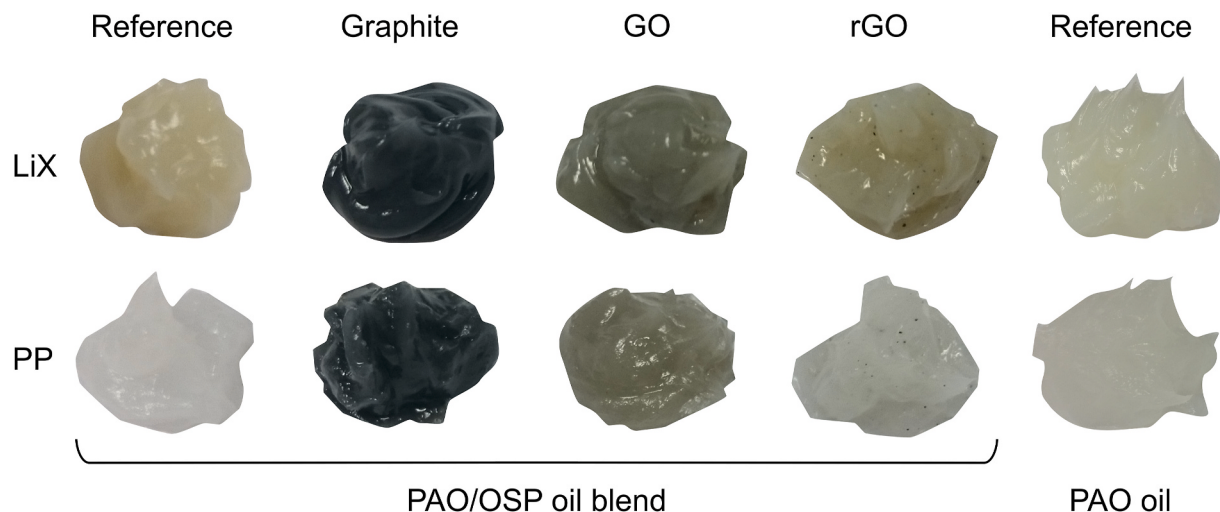


Fig. 2. Images of the eight different manufactured PAO/OSP greases without (reference) and with additives (0.1 wt% graphite, GO and rGO, respectively) for the two thickener systems, LiX and PP. The LiX and PP PAO reference greases, without additives as in Ref. [39], are shown to the right.

electron microscope (SEM, Zeiss Merlin). The thickener samples were prepared by the following procedure: A thin layer of grease was applied to a woven stainless-steel wire cloth (Derma AB) with a wire diameter of 67 μm and an aperture width (the width between the wires) of 100 μm . The wire cloth had been ultrasonically cleaned for 5 min in hexane and ethanol, respectively, before grease application. Hexane was then slowly dropped onto the grease for a few minutes to remove the oil, i.e., about 80–90% of the grease. Whether and how hexane affects the thickener structure was not investigated. However, hexane, toluene and petroleum ether have all been used previously to remove the oil before SEM analysis of grease thickener structures [43–46]. The thickener left on the wire cloth after oil removal had a white powdery appearance. A separate wire cloth was used for each grease type. After removing the oil, the thickener samples were sputter coated with Au/Pd to enhance their

conductivity before the SEM analysis. The SEM analysis was performed with an electron acceleration voltage of 5 kV.

2.2. Test setup and materials

Several different experiments were conducted to investigate the lubricating potential of the additives. Fretting tests were performed since fretting is a common tribological problem in power connector applications. The contact situation was varied from fretting of crossed cylinders to continuous motion in 4-ball tests to investigate the influence of contact geometry and motion, as well as of material combination. The experimental details are summarized in Tables 3 and 4.

Table 3

Experiments performed to investigate the lubricating performance of the greases under different contact conditions and material combinations.

Test	Contact materials	Lubrication	Aim
Fretting	Silver-coated copper	Grease with and without additives	Investigate influence of additives in a grease-lubricated Ag/Cu versus Ag/Cu contact in fretting
4-ball Wear scar	Steel	Grease with and without additives	Investigate friction and wear of the balls for greases with and without additives in a 4-ball steel/steel contact
4-ball Last non-seizure load	Steel	Grease with and without additives	Investigate the last non-seizure load for greases with and without additives in a 4-ball steel/steel contact

Table 4

Test parameters for the performed experiments. Note that all tests are performed at room temperature, i.e., no external heating was used.

Parameter	Type of test	4-ball
	Fretting	
Contact geometry	Crossed cylinders (perpendicular)	One ball on top of three others
Material	Silver-coated copper	Steel (AISI 52100)
Sample dimensions	10 mm in diameter, 20 mm long	12.7 mm in diameter
Displacement amplitude	$\pm 50 \mu\text{m}$ and $\pm 200 \mu\text{m}$	–
Sliding length per revolution	–	23.1 mm
Number of cycles or revolutions	100 000	6240 (wear scar)
Frequency of motion [Hz]	100	–
Rotational speed [rpm]	–	104 (wear scar)
Current load [A] d.c	10	1450 (last non-seizure load)
Applied normal load [N]	50	–
Hertzian maximum contact pressure [GPa]	1.21 ^a	400 (wear scar) >200 (last non-seizure load) 3.49 ^b (wear scar)

^a Calculated for typical copper properties: $E = 120 \text{ GPa}$ and $\nu = 0.33$.

^b Calculated for typical steel properties: $E = 213 \text{ GPa}$ and $\nu = 0.29$. The load in each of the three contact points is the applied normal load divided by $\sqrt{6}$. In the case of 4-ball wear scar tests the contact pressure is approximated for two vertically aligned spheres.

2.2.1. Fretting tests

The fretting experiments were conducted in the same equipment as in Ref. [39]. Two perpendicularly crossed silver-coated copper (Ag/Cu) cylinders (10×20 mm) were used to simulate an electrical contact. The lower cylinder is mounted on a vibrating table that vibrates back and forth (the cylinder axis is parallel to the vibration direction), while the top cylinder is fixed. The tangential force, the vibration of the table and the contact resistance were continuously recorded during the tests. The silver coating on the copper cylinders was about $20 \mu\text{m}$ thick and the surface roughness, S_a , about $0.27 \mu\text{m}$ based on several measurements on the coating surface. The contacts were tested lubricated with the LiX and PP greases with and without graphite, GO and rGO. Before the first test, the cylinders were ultrasonically cleaned, 5 min each in acetone and ethanol. The cylinders were cleaned with ethanol between repeated tests using the same cylinders. Several tests were made on the same cylinder pair after rotating to expose unaffected contact surfaces. Grease was applied in excess on the lower cylinder before the two cylinders were pressed into contact and the fretting motion was started.

2.2.2. 4-ball wear scar and seizure tests

A tribometer with a sliding 4-ball setup (Rtec Instruments, MFT-5000) was utilized to further examine the greases. Three chrome alloy steel balls (AISI 52100) with a diameter of 12.7 mm were held together and inserted into a cup filled with grease. The fourth ball was fixed and attached to a motor that presses and rotates the ball on top of the three others. The friction and temperature were recorded during the test. The standard DIN 51350:1 [47], describes the general working principles of a 4-ball test.

The grease was evaluated for a specific applied load, speed and test length to determine the effect of the additives on friction and wear. For detailed information of test parameters, see section 2.3. The wear scar diameter was measured on the bottom balls after the tests. The wear scar diameter together with the friction results were used to compare the greases. This type of test is called 4-ball wear scar. A similar procedure, but with a ramped applied load, served to investigate the influence of the additive on the last non-seizure load. The last non-seizure load is characterized by a sudden increase of the friction coefficient. The load was ramped up until this drastic increase, at which point the test was stopped. No weld was formed between the upper and bottom balls.

2.3. Test parameters

The fretting experiments were conducted at pre-set displacement amplitudes $\pm 50 \mu\text{m}$ and $\pm 200 \mu\text{m}$ (100 and 400 μm peak-to-peak amplitude, respectively), with 50 N applied normal load and a frequency of 100 Hz, based on the results found in Ref. [39]. The previous study also included $\pm 25 \mu\text{m}$. However, this was found less interesting since the grease-lubricated Ag/Cu contacts behaved almost as if unlubricated at such a small amplitude. The grease was rapidly pushed out of the contact, resulting in permanent welding of the two cylinders.

The pre-set displacement amplitude is the vibration amplitude set to the table without the resistance of the friction, i.e., the amplitude before the two cylinders are pressed into contact. Since the test is force controlled rather than displacement controlled, the amplitude of the table will always be reduced due to the friction forces during testing. The higher the friction force, the larger the reduction in amplitude. Hence, the actual displacement amplitude of the vibrating table cannot exceed the pre-set value. The fretting tests for each grease type were conducted twice. Test parameter details are listed in Table 4.

Each 4-ball test was run for 60 min without external heating. For the wear scar tests the load and rotational speed was 400 N and 104 rpm (corresponding to 40 mm/s of sliding, which is half the sliding distance per second in the fretting tests, at a displacement of $\pm 200 \mu\text{m}$). The 4-ball wear scar tests were conducted three times for each grease type. The last non-seizure load tests were run at 1450 rpm with a linearly increasing applied load. The load was ramped 1.35 N per second,

starting from 200 N, until the friction drastically increased indicating the lubricating grease film breakthrough. Three tests were performed per grease type. The test parameters are presented in Table 4.

2.4. Surface analysis

Scanning electron microscopy (SEM, Zeiss Merlin), energy dispersive X-ray spectroscopy (EDS, Oxford X-max), and vertical scanning interferometry (VSI, Zyglo Nexview) were used to analyze the surfaces after the fretting experiments. The acceleration voltage during EDS analysis was 10 kV. The samples were cleaned with hexane and ethanol in an ultrasonic bath 5 min in each solution prior to analysis.

A light optical microscope (LOM) was used to determine the wear scar diameter on all bottom balls from the 4-ball wear scar tests. One of the three bottom balls from each grease type tested was further analyzed with VSI, SEM and EDS. The acceleration voltage during EDS analysis was 5 kV.

3. Results

3.1. Grease thickener structure analysis

The structure of the four reference greases was investigated in the SEM, after washing out the oil. The LiX PAO reference thickener, Fig. 3b, is composed of many short, thin entangled, densely arranged fibers. Similar structure regions were found also for the LiX PAO/OSP reference grease, but most of the analyzed structure has a more continuous fiber-network appearance, as illustrated in Fig. 3a. The PP thickener produces thicker fibers than the corresponding LiX thickener. Clearly, the oil blend type and the thickener type together influence the grease thickener structure.

3.2. Fretting tests

In the fretting tests, the additives showed no or only a small positive effect on the coefficient of friction compared with the reference grease without additives. This is true for both displacement amplitudes, see Figs. 4 and 6. Similarly, no positive effect of the additives was noted on the wear marks (Fig. 5).

3.2.1. Fretting at pre-set displacement amplitude $\pm 50 \mu\text{m}$

When testing with the $\pm 50 \mu\text{m}$ amplitude, the coefficient of friction is slightly lower for the LiX greases with additives than for the LiX PAO/OSP reference grease, see Fig. 4a. The LiX PAO reference grease results in lower or similar friction than the PAO/OSP greases with and without additives. The high friction in the beginning of the LiX-grease tests are due to welding of the cylinders and the friction drop occurs when the weld breaks [39]. Further, the contact resistance was similar for all tests, 20–30 $\mu\Omega$ for the PAO/OSP greases and slightly higher, 40 $\mu\Omega$ for the PAO reference grease (Fig. 4c).

The coefficient of friction (0.08–0.1) and contact resistance (20–30 $\mu\Omega$) were similar for all the PP greases regardless of additives and oil blend type, see Fig. 4b and d.

Within a single thickener system, the wear marks on the cylinders showed similar appearance, with no visible effects from running with or without additives. The wear marks from the LiX-lubricated tests (approximately 900 μm in the vibration direction and 700 μm in the perpendicular direction) were somewhat larger than those from the corresponding PP-lubricated tests (approximately 800 μm and 600 μm in the vibration and perpendicular direction, respectively), see Fig. 5a and b. This difference is a result of the more extensive contact area growth during the initial welded period of the LiX-lubricated surfaces compared with that during sliding of PP-lubricated surfaces. Note that PP-lubricated contacts also start at a high friction level, but in this case for a very short time before rapidly reaching low stable friction. The welding and weld breaking phenomena were described in Ref. [39].

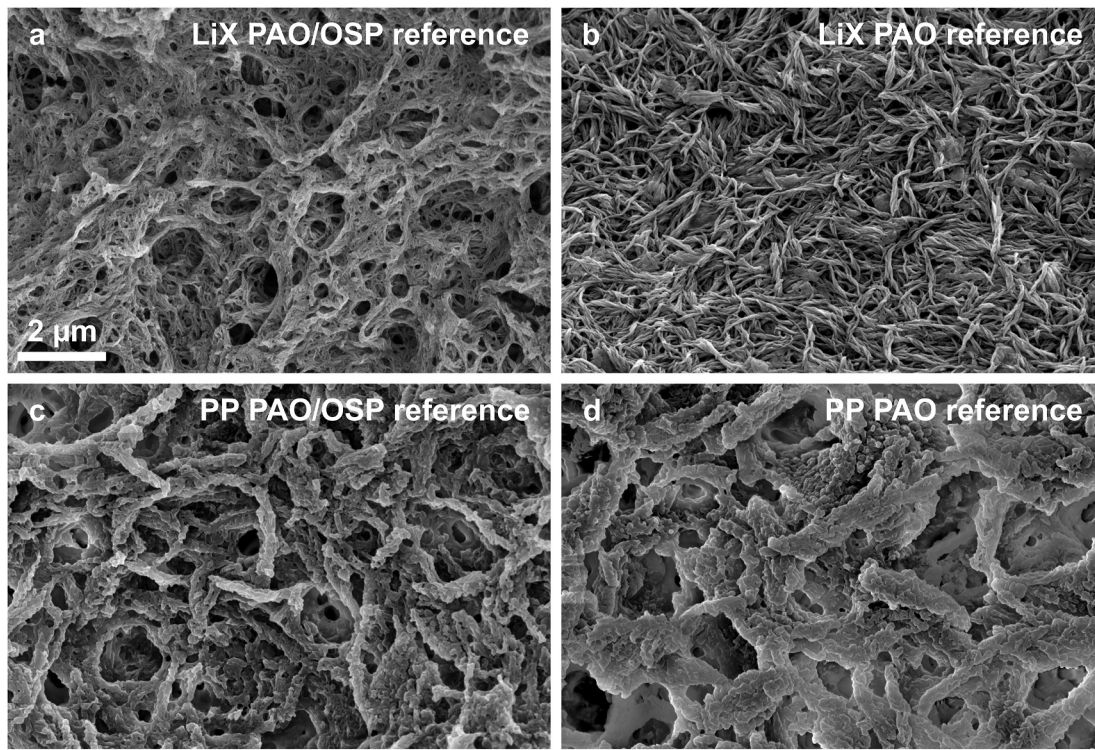


Fig. 3. SEM images of the thickener microstructure for the following base greases: a) LiX PAO/OSP reference thickener, b) LiX PAO reference thickener c) and d) the same as in a) and b) but with PP thickener. The scale bar in a) is valid for all images in Fig. 3.

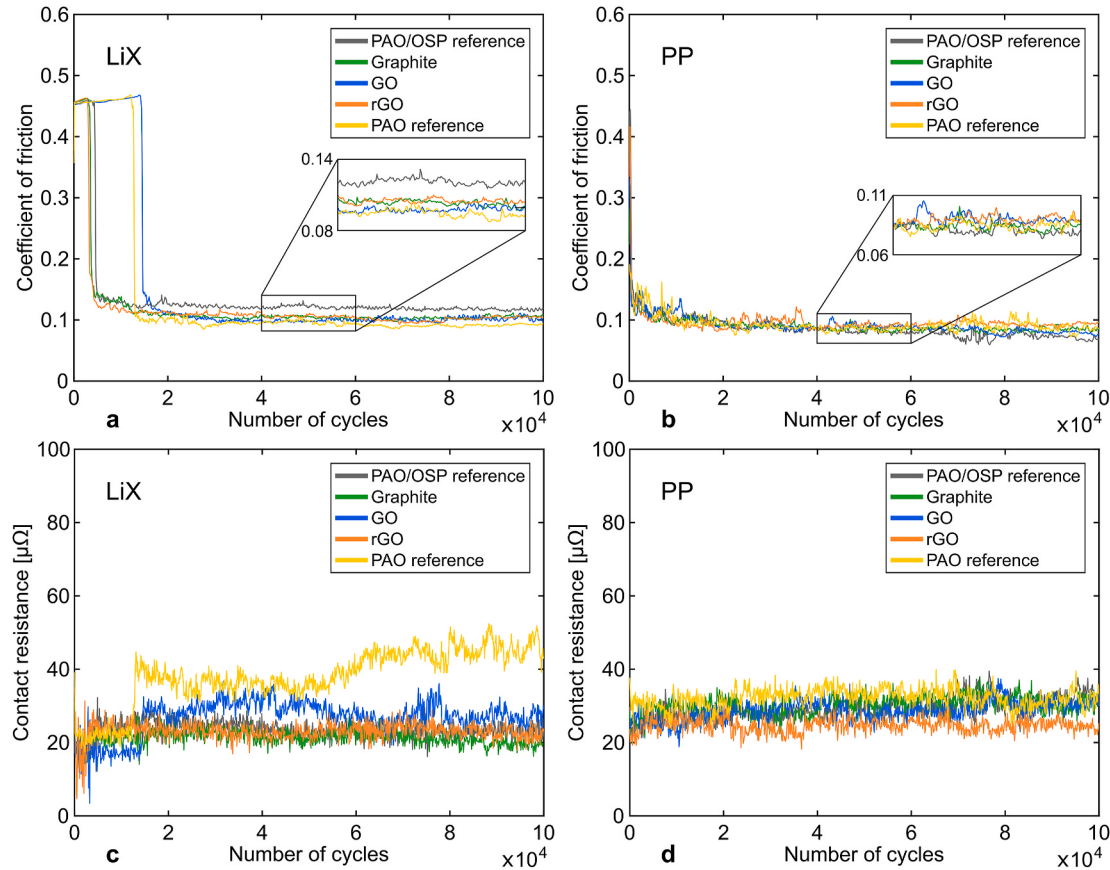


Fig. 4. Friction coefficient and contact resistance curves from fretting of Ag/Cu versus Ag/Cu, with a pre-set displacement amplitude of ±50 μm. Top row: Coefficient of friction. Bottom row: Contact resistance. Only one graph per grease type is presented here since all test repetitions showed similar result. a) and c) LiX greases and b) and d) PP greases. (PAO/OSP oil blend unless other stated).

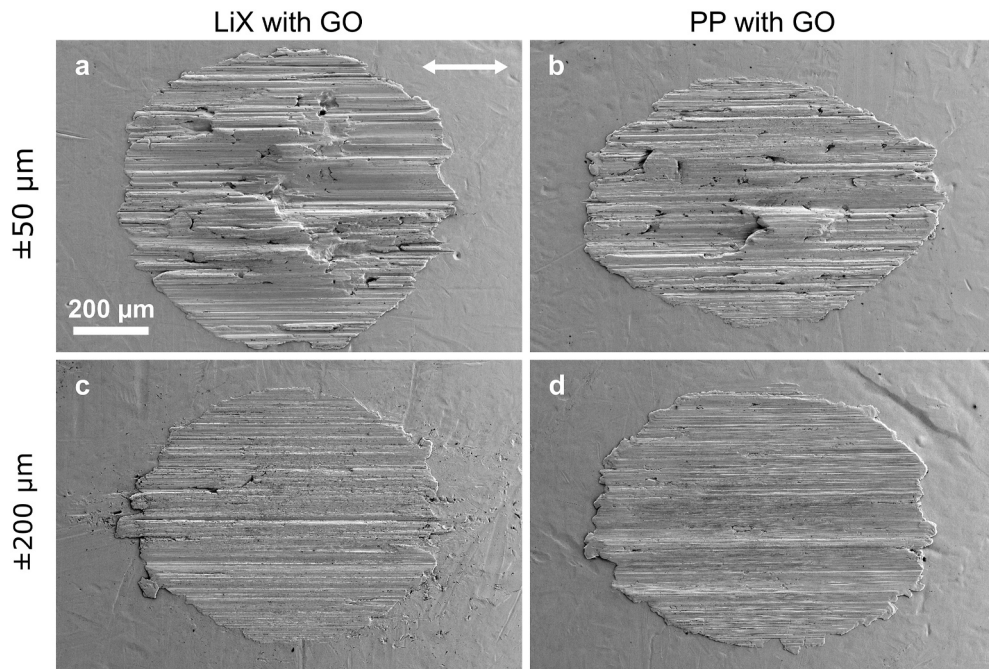


Fig. 5. SEM images of the contact areas on the stationary Ag/Cu cylinder from fretting tests lubricated with LiX and PP PAO/OSP greases with GO. The cylinder axis is perpendicular to the vibration direction. Vibration direction \leftrightarrow of the vibrating countersurface and scale bar as indicated in a). a) Pre-set displacement amplitude of $\pm 50 \mu\text{m}$ and LiX grease, b) $\pm 50 \mu\text{m}$ and PP grease, c) $\pm 200 \mu\text{m}$ and LiX grease and d) $\pm 200 \mu\text{m}$ and PP grease. The wear marks in a, b, c and d, respectively, were approximately 880, 930, 800 and 880 μm in the vibration direction and 800, 640, 670 and 670 μm in the perpendicular direction.

Copper was exposed on the stationary cylinder for all LiX-lubricated tests (as evident from EDS-results not shown). For PP-lubricated contacts, the grease with GO and rGO resulted in exposed copper on the stationary cylinder, but to a lesser degree than for the LiX grease.

3.2.2. Fretting at pre-set displacement amplitude $\pm 200 \mu\text{m}$

At the $\pm 200 \mu\text{m}$ displacement amplitude the friction typically differs

between parallel tests with the same LiX grease (Fig. 6a). This is especially true for the greases with graphite and GO. In general, the coefficient of friction is slightly lower for the LiX-lubricated contacts than for the PP-lubricated (Fig. 6a and b). The contact resistance is about 100–200 $\mu\Omega$ and 50–100 $\mu\Omega$ for surfaces lubricated with LiX and PP grease, respectively (Fig. 6c and d). The wear mark appearances are similar for all grease-lubricated tests, see Fig. 5c and d. The wear mark

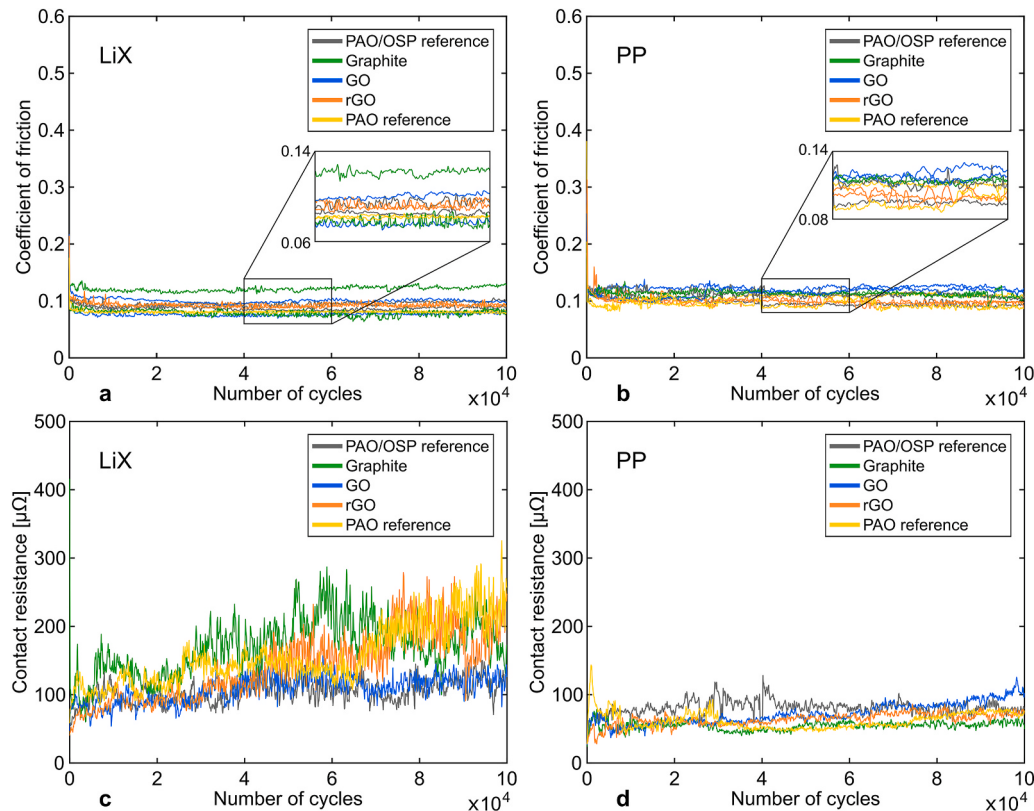


Fig. 6. Friction coefficient and contact resistance curves from fretting of Ag/Cu versus Ag/Cu, with a pre-set displacement amplitude of $\pm 200 \mu\text{m}$. Top row: Coefficient of friction. Two curves per grease type are presented to illustrate the spread between test repetitions, especially for the PAO/OSP greases with graphite and GO, respectively. Bottom row: Contact resistance (one curve per grease). a) and c) LiX greases and b) and d) PP greases. (PAO/OSP oil blend unless other stated).

diameters in the vibration direction were about 800 µm for LiX greases and about 880 µm for PP greases. The diameter in the perpendicular direction was about 700 µm for both LiX- and PP-lubricated tests. No or only low copper signal was detected in the wear marks on the stationary cylinders for the LiX- and PP-lubricated contacts (EDS-results not shown).

The PAO reference greases show lower or equivalent friction levels as the PAO/OSP greases, see Fig. 6a and b. Neither GO nor rGO additives give better performance than graphite in the fretting tests.

3.3. 4-ball wear scar and seizure tests

The 4-ball tests show no significant friction difference (95% confidence interval) between the ten different greases (Fig. 7a and b).

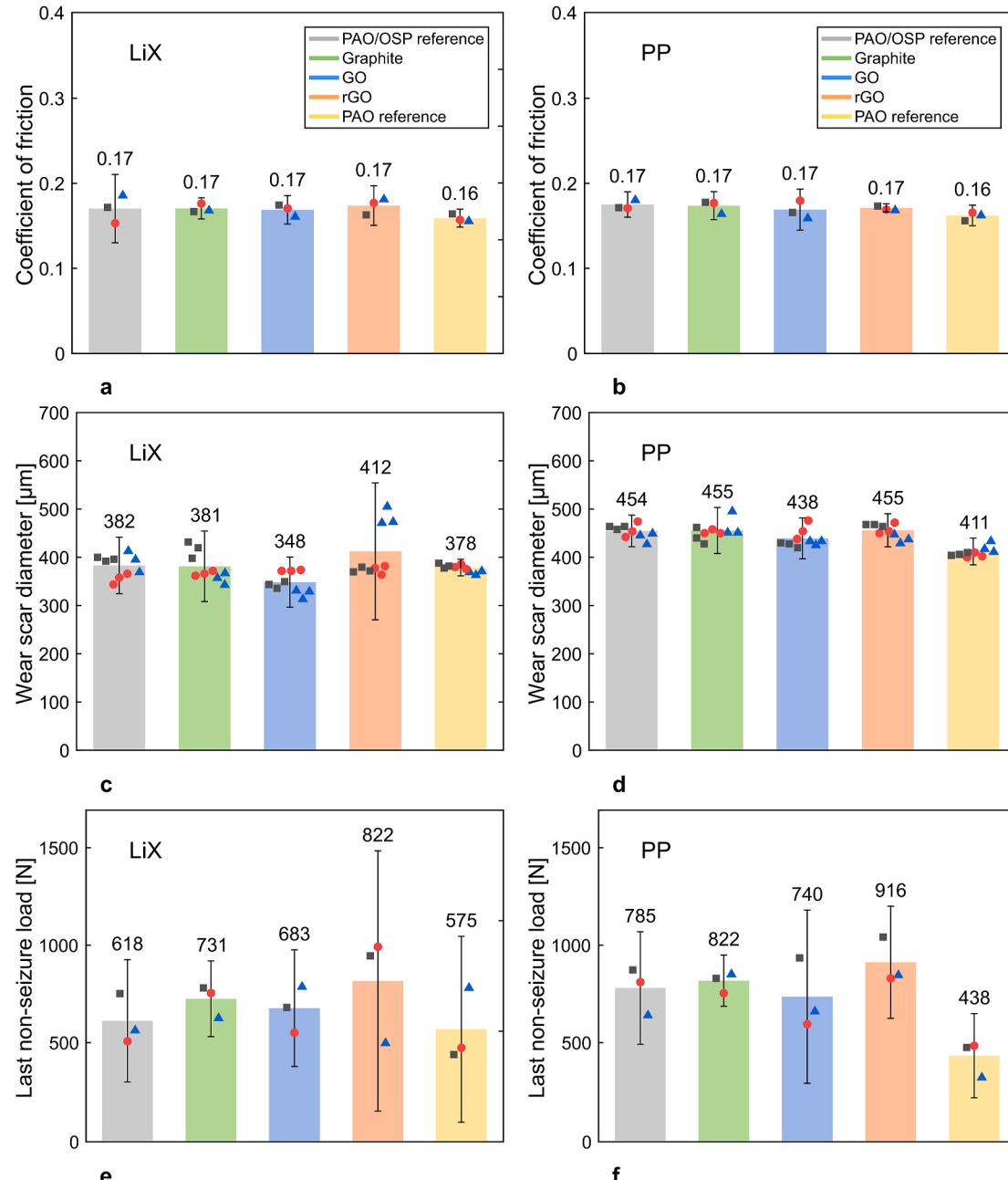


Fig. 7. Friction and wear results from the LiX and PP grease-lubricated 4-ball experiments, steel versus steel. The graphs show the average values (bar height and included numbers), the value for each parallel test (indicated by (square, circle and triangle) and the 95% confidence intervals. (PAO/OSP oil blend unless other stated). a) and b) Coefficient of friction, three parallel tests. c) and d) Wear scar diameter (mean of the nine bottom balls for each grease type). e) and f) Last non-seizure load, three parallel tests. Note that the tests were stopped when the friction drastically increased and before any welding between the top and bottom balls occurred.

In general, the spread is large between test repetitions and the confidence intervals overlap for almost all greases. The PP PAO reference grease shows the lowest mean last non-seizure load. Interestingly, the PAO reference greases, which showed the lowest mean friction and a quite small wear scar diameter, also shows the lowest mean last non-seizure load, in both the LiX (575 ± 192 N) and the PP version (438 ± 88 N).

The wear mark on one of the bottom balls from tests with each of the LiX and PP greases are presented in Figs. 8 and 9. The wear marks from the LiX-lubricated tests are smaller, and show less surface damage, than the corresponding PP-lubricated. PP wear marks show both more wear on the ball (size of the pits in Fig. 9) and more formed tribofilms. Most of the dark lines in the wear marks in Fig. 8a–e are scratches, while the dark areas found in the marks in Fig. 8f–j are both scratches and tribofilms based on iron, oxygen and carbon. This is based on the SEM and EDS analysis of the wear marks, and is thereby not evident from Fig. 8. As mentioned, the surfaces lubricated with PP grease generally show more of these tribofilms than those lubricated with LiX grease, as demonstrated by the examples in Fig. 10a and b. Also greases without the carbon-based additives show a higher carbon signal inside than outside of the wear mark (results not shown). This means that it is not possible to say if the carbon-based additives are part of the tribofilms based on EDS as analysis method. Further, oxygen is present as an iron oxide, see Fig. 11, and often together with carbon in regions close to the iron oxide tribofilms. The oxygen- and carbon-rich films are most likely formed from the grease constituents (thickener and/or oil). The carbon signal sometimes also coheres with the iron oxide tribofilms, indicating that the grease constituents form films both on and beside iron oxide regions.

4. Discussion

In the present study, none of the graphite, GO or rGO additives reduced the friction or wear from the levels of the reference greases. This was true in both the fretting and 4-ball tests. Hence, these types of lubricating additives in greases do not guarantee a reduction of friction and wear. Further, the additives showed no clear effect on the contact resistance in the fretting tests of silver-coated copper cylinders simulating electrical contacts. The following discussion is intended to elucidate the complexity of graphene-based materials in greases in tribological contacts and to discuss why the effects were so insignificant in the present investigation.

4.1. About additives

4.1.1. Additive concentration

One reason behind the insignificant effects of the additives, might be that the additive concentration is too low or too high. In the literature, numerous authors have found optimal additive concentrations for their studied tribological contacts including 4-ball as well as reciprocating and continuous sliding ball-on-disc tests under varying contact conditions [5–9,12–15,21,22,24,32,48,49]. At low concentrations, the wear protection is not sufficient and at high concentrations, the large number of additive particles in oil or grease may hinder the formation of a completely covering oil film protecting the surfaces, eventually causing the surfaces to run dry [48,49]. The additive concentration chosen in the present study is lower than the additive concentration optima of 0.3 and 0.5 wt% GO used in oils [21,22], and lower than 0.4 wt% rGO [24] and 3 wt% graphene in grease [9]. The chosen concentration of 0.1 wt% is, however, the same as the concentration optimum found for graphene in bentone and lithium grease, respectively, [8,14]. Zhang et al. [49] found that oil with 0.06 wt% graphene was optimal for enhanced friction and anti-wear performance. Lin et al. [5] reported that 0.075 wt% modified graphene platelets clearly improved the wear resistance and the load carrying capacity in oil. Powdered graphite and molybdenum disulphide in a concentration of 10% in grease were effective as anti-wear additives in fretting tests by Neyman and Sikora [50], while concentrations of 1, 3 and 5% were not effective. From this, it is clear that the optimum additive concentration varies with parameters such as additive type and the matrix it is added to. The chosen tribological evaluation method is also an important factor, which most certainly will influence the additive's chances of reducing friction and wear. A complete mapping of the concentration optima for graphite, GO and rGO in greases would shed more light on their lubricating potentials with respect to e.g., friction, wear, and last non-seizure load. After an optimization for each additive, a fairer comparison between the additives in the greases can be performed. Such optimization is beyond the scope of the present study.

4.1.2. The additives need to reach the surfaces

Another reason to why no friction and wear reduction effects of the additives were found, might be that they simply do not reach the rubbing surfaces. In the work by Huang et al. [32], graphite nanosheets in paraffin oil was superior to flake graphite in the same oil to reduce the friction and wear scar size, as well as to increase the maximum non-seized load, i.e., the oil load bearing capacity of the oil. This

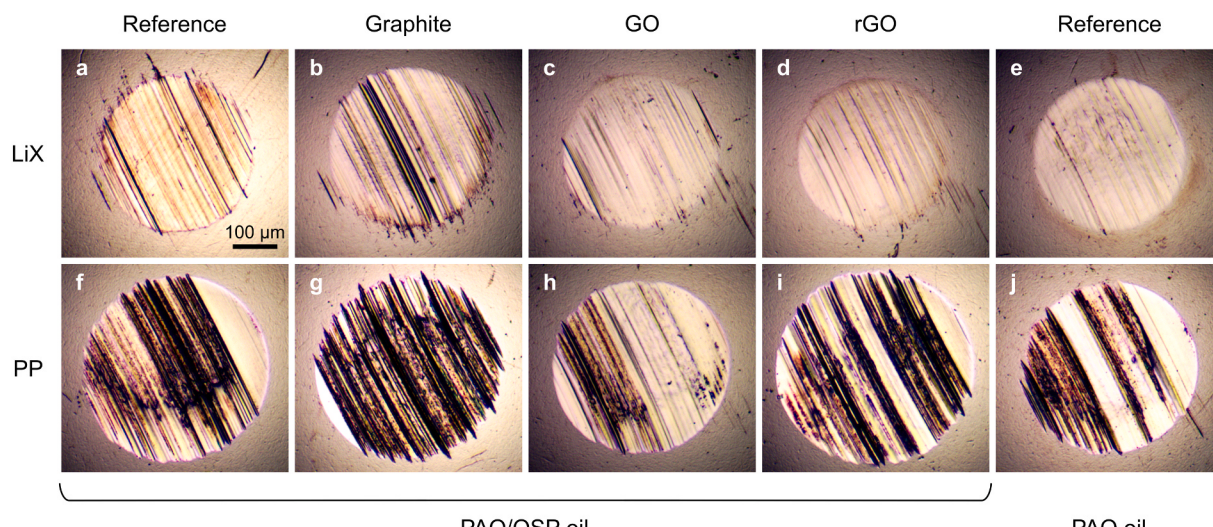


Fig. 8. Wear mark appearances after grease-lubricated 4-ball experiments, steel versus steel. LOM images showing one bottom ball for each grease type, as presented in Table 1. a–e) LiX greases, f–j) PP greases. The scale bar in a) is valid for all wear marks in Fig. 8. The wear marks in a–e) are approximately 360, 360, 350, 340 and 340 μm in diameter. The corresponding sizes of wear marks in f–j) are 410, 430, 400, 480 and 390 μm .

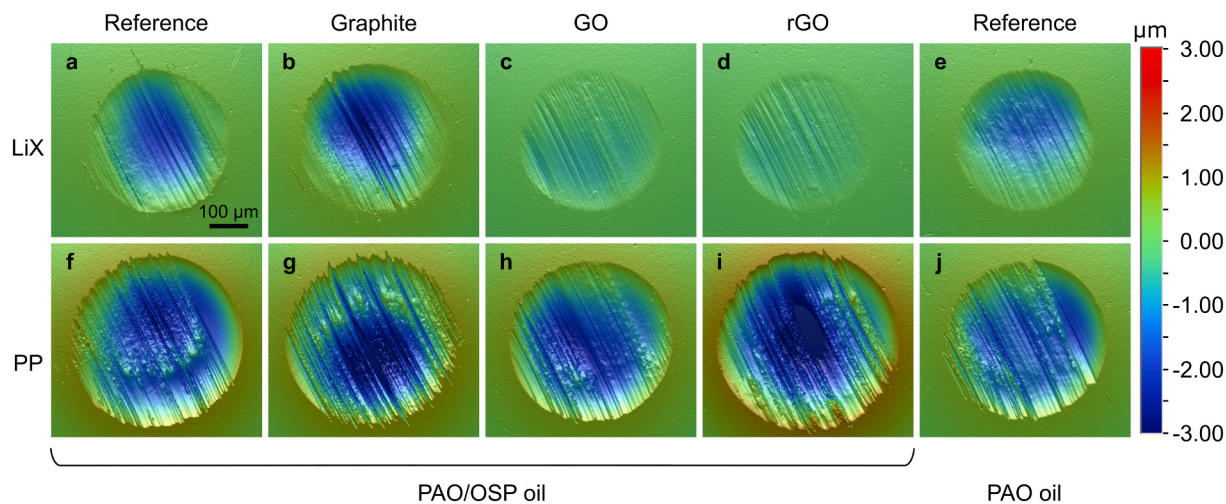


Fig. 9. Wear mark shapes after the grease-lubricated 4-ball experiments, steel versus steel. VSI images showing one bottom ball for each grease type presented in Table 1 (the same scars as in Fig. 8). The VSI software has here compensated for the spherical shape of the ball, hence the almost flat wear mark on the ball appears as a shallow pit in a flat surface. a-e) LiX greases. f-j) PP greases. The scale bar in a) is valid for all wear marks in Fig. 9.

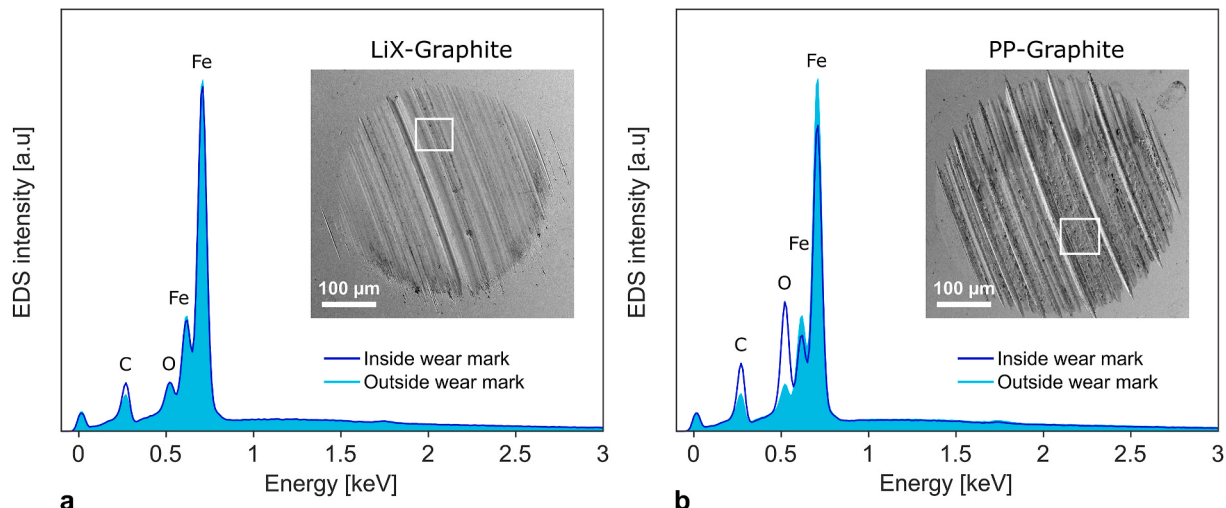


Fig. 10. Appearance and surface analysis of wear scars generated in grease-lubricated 4-ball wear scar experiments, steel versus steel. EDS spectra in and outside the wear mark on one of the bottom balls for a) LiX PAO/OSP grease with graphite, here called LiX-Graphite and b) PP PAO/OSP grease with graphite, called PP-Graphite. The white box in each SEM image indicates where the EDS spectrum was recorded. The wear marks in a) and b) are the same as was presented for the specific greases in Figs. 8 and 9.

indicates that the particle size of the additive is an important parameter. Larger particles are probably more easily pushed out from the contact and/or tend not to enter it as easily as smaller particles do. A longer sonication time of the additives in oil could possibly further exfoliate the graphene-based sheets in the produced greases. However, an excessively long sonication time can result in sheet size reduction and introduction of defects [33]. A more detailed surface investigation is needed to learn if the graphene-based additives in the present study create tribofilms on the surfaces in the fretting and 4-ball tests. Further, the sonication procedure could probably be improved to enhance the additive dispersion.

4.1.3. GO and rGO quality

The quality of GO and rGO (here used as received) could also be an important factor. According to Kauling et al. [30], many graphene producers sell fine graphite instead of graphene. For future development of greases with GO, it is important to have better specified raw materials (purity, size, thickness, etc.). The new standard from 2021 [31], which includes methods for characterizing the structural properties of

graphene from powders and liquid dispersions, is an important tool for users to know what material they are working with. However, this standard does not include purity determination methods.

4.1.4. Contact pressure

The contact pressure, and thereby the applied contact load, is another aspect to consider for the lubricating effect and the possibility to find additive tribofilms on the surfaces after test. Wang et al. [11], Fu et al. [13] and Li et al. [14] report that the lubricating role of graphene varies with the applied contact load. Using Raman spectroscopy, no graphene was detected on the surfaces from reciprocating ball-on-disc tests at 100 N, but was detected for loads of 200 and 400 N [11]. The graphene peak intensity was lower after the 400 N than after the 200 N test, due to tribofilm destruction at high loads. These results indicate that a certain contact pressure is needed for graphene to take part in the lubrication and that at even higher pressures, the formed graphene-containing tribofilms can be destructed. Although these results were found for graphene, it is possible that also the lubricating effect of graphite, GO and rGO varies in a similar way (since all these

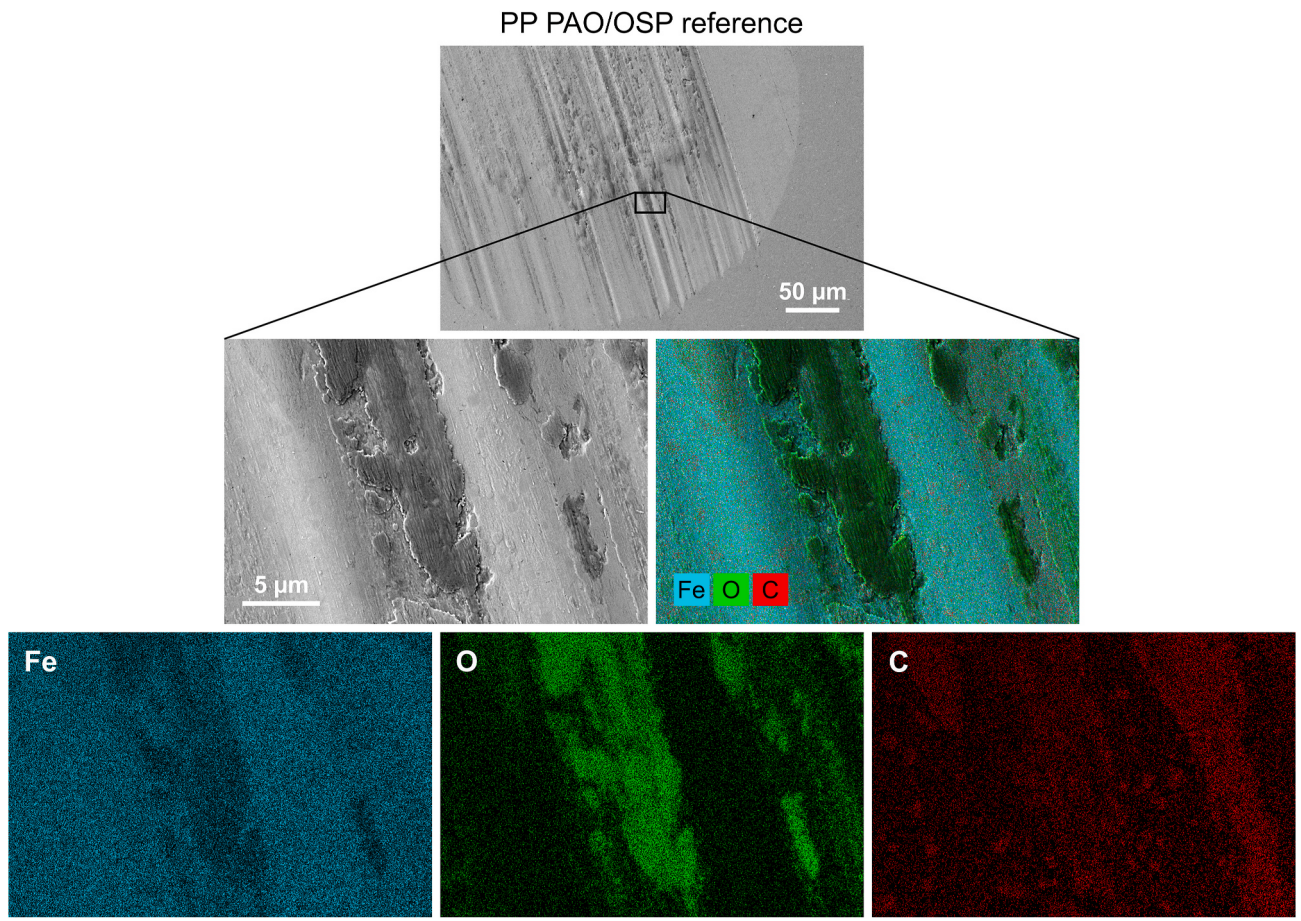


Fig. 11. Example of surface appearance (SEM) and elemental composition (EDS mapping) of a wear mark on a bottom ball from a 4-ball test with the PP PAO/OSP reference grease (the same wear mark as in Figs. 8f and 9f). Top: overview of the wear scar. Middle row: Detail showing tribofilm formation (darker), SEM + EDS mapping overlay. Bottom row: separate EDS maps showing the distribution of Fe, O, and C. The black box in the top image shows the position of the details below.

materials, except from single-layer graphene/GO/rGO, have a layered structure, which most certainly result in similar lubricating mechanisms).

4.2. Greases developed for this study

4.2.1. Additive response and friction characteristics of LiX and PP greases

Based on previous results, the PP grease was expected to result in better additive response and thereby lower friction than the LiX grease [35,37,38,51]. No such response was found in the present study. In fretting at high displacement amplitudes, LiX greases generally gives lower friction than PP greases (Fig. 6) and all greases result in similar friction levels in 4-ball wear scar tests regardless of thickener type (Fig. 7a and b). This holds true for the reference greases as well as the greases with additives. The fact that the LiX reference grease provides lower friction than the PP reference grease has been noted in previous grease investigations, when the contact pair is in the gross slip fretting regime [39].

In bearing tests [51], PP grease was found to require longer time than LiX grease to reach a steady state level of friction. After a running-in period (of around 7 days), the temperature of the PP grease generally fluctuated less than that of the corresponding LiX grease (the temperature was measured on two positions on the outer ring of each bearing). The long polypropylene molecules degraded into smaller molecular species due to high shear forces. These PP fractions have boundary friction reducing properties. The fretting tests in the present study, are probably too short to form a large enough number of PP fractions to reduce the friction as found in Ref. [51].

The two oil types used for the presently evaluated greases (PAO and OSP) vary slightly in viscosity. However, calculating the base oil viscosity according to ASTM D7152 [52] indicates only a small difference between the PAO/OSP oil blend and the PAO oil. This small difference is not believed to explain the difference in friction level between the LiX PAO/OSP reference grease and the LiX PAO reference grease in Fig. 4a. If the variation in viscosity would be a contributing factor to the friction results, this effect would have been seen also for the PP reference greases in Fig. 4b, but this is not the case.

The chosen concentration of graphite, GO and rGO in this study is sufficiently low to not expect it to cause a significant effect on the grease consistency. However, the small amount of extra oil that was mixed into the greases together with the additives may have caused a slight decrease in consistency. Since no corresponding oil was added to the base reference greases, the greases with and without additives could vary slightly in consistency. Based on the friction results, this difference has not significantly affected the results.

4.2.2. Choice of base oil

It has been shown that both 5 and 10% of OSP in pure PAO-8 oil reduce the friction in a steel/steel contact compared with the pure PAO-8, when evaluated in a mini-traction machine [53]. The largest reduction was noted for 10% OSP. But in the present work, as shown in Figs. 4, 6 and 7, the PAO reference greases often show the lowest friction. Therefore, it may be more cost effective to choose a base oil/thickener system that results in lower friction completely without additives, instead of producing a grease with an oil blend specifically chosen to facilitate the additive dispersion. Based on the friction results in the

present study, it would be interesting to evaluate the lubricating effect of the additives in PAO greases. A more comprehensive graphite/GO/rGO/grease study (with respect to better specified raw materials, additive concentration, as well as optimizing the sonication procedure of the additives in oil) would be helpful to clarify if addition of the lubricating additives is cost efficient and actually results in reduced friction and wear.

4.2.3. Grease thickener structure

The lubricating film thickness is determined by a combined effect of thickener, oil type and oil viscosity [49,54,55]. Parameters such as soap concentration, cooling rate (during grease manufacturing), base oil viscosity and base oil type, all influence soap-thickener structures [43, 56,57]. The manufacturing parameters are important also for the resulting PP-thickener structure. Based on this and that the fiber structures differed between the greases with different base oil and thickener types (Fig. 3), it is not surprising that the friction results differ slightly between the PAO and PAO/OSP reference greases. The oil-removal procedure needed to reveal the fiber structures in Fig. 3 may have affected, and further, these structures likely become degraded by the heavy shear deformation in the tribological testing. Nevertheless, the SEM images serve as a valuable comparison between the different greases.

4.3. Tribological results

4.3.1. Appearance and tribofilm formation of 4-ball wear scar tested surfaces

The wear scars on steel balls (from the 4-ball wear scar tests) lubricated with PP greases show more iron oxide regions and more oxygen- and carbon-rich tribofilms than those lubricated with LiX greases, independent of base oil blend (Figs. 10 and 11). The statistically significant difference in wear between the two thickener types, LiX and PP, is important for future grease development and testing. In the present study, the choice of thickener proved to be more important for the lubricating properties of the grease, than was the addition of graphite, GO or rGO additives. The only difference between the LiX and PP greases manufactured with the same base oil blend is related to the thickener. Since the PP-lubricated contacts are more oxidized and more affected from the 4-ball test than the corresponding LiX-lubricated contacts, it can be concluded that there is more metal-to-metal contact during these tests even though the resulting coefficient of friction is the same. This must mean that the lubricating films of the LiX greases more efficiently protects the surfaces than the films formed with the PP greases, under the prevailing contact conditions. The mechanisms behind the difference between LiX and PP greases are not yet fully understood, so more detailed investigations will be needed. The greases evaluated here do not contain any antioxidants or other types of additives as in the commercial greases. Hence, the results for commercial LiX and PP greases may differ from what have been seen here.

From X-ray photoelectron spectroscopy (XPS) analysis, Wang et al. [11] suggested that the addition of graphene in lithium grease not only reduces the friction and wear compared with the base grease without graphene, but also promotes the formation of Fe_2O_3 and Li_2O tribofilms on the tested steel surfaces. Deposited graphene together with Fe_2O_3 and Li_2O tribofilms were stated to improve the tribological properties of the grease. In the present study, XPS analysis in and outside the wear marks on steel balls lubricated with LiX- and PP PAO reference grease was performed (results not shown). Lithium could not be detected on the surface lubricated with LiX grease. Note that this does not necessarily mean that there is no lithium on the surface. The hypothesis before analysis was that the tribofilms on LiX-lubricated steel surfaces would involve lithium and that these could be the reason for the better surface protection compared with PP grease. XPS analysis of lithium is normally challenging, since the sensitivity is low [58] and there are no other peaks than Li1s that can assist in data interpretation. An additional

complicating factor in the case of finding lithium on steel surfaces, except for the low sensitivity, is that the Li1s and Fe3p peaks overlap. Peak fitting is required to detect a lithium contribution. The authors of the present paper do not agree with the conclusions drawn by Wang et al. [11] regarding their XPS data, and believe that they have mistakenly interpreted the Fe3p signal as Li1s. A reference measurement of Fe3p outside the wear mark on the tested steel surface would show if there is a Li1s contribution in the wear mark or not. This was not included in their paper.

4.3.2. 4-Ball seizure tests

The last non-seizure load tests (4-ball seizure tests) show a large spread between tests with the same grease. The last non-seizure loads found here are quite low compared with the ones found for greases with extreme pressure additives such as ZDDP (zinc dithiophosphate). Greases with weld loads below and above 2500 N are considered as having no, and some, extreme pressure functionality, respectively. The application determines the weld load needed, and a weld load of 2500–3200 N is often enough for bearings. The results suggest that graphite and graphene-based materials do not work as extreme pressure additives in the formulated greases of this study. However, they might work better when the properties of the additives, oil and thickener have been optimized.

4.3.3. LiX and PP grease in fretting of power connectors

Generally, grease protects the surfaces from wear and reduces the coefficient of friction to a low and stable level. Both LiX- and PP-lubricated surfaces result in a contact resistance of about 20–40 $\mu\Omega$ at a pre-set displacement amplitude of $\pm 50 \mu\text{m}$ and 50 N load, which is acceptable for power connectors (Fig. 4). However, at $\pm 200 \mu\text{m}$ the contact resistance of LiX-lubricated surfaces is unacceptably high (100–200 $\mu\Omega$), and would cause large energy losses in power connectors (Fig. 6). The PP-lubricated contacts also show high contact resistance values (50–100 $\mu\Omega$), but more acceptable than LiX. At this high vibration amplitude, the contact resistance increases throughout the tests with LiX grease, which means that the surfaces become more and more electrically separated. More separated surfaces result in less contact points able to transport current. The reason behind the increased resistance is not yet understood but could be linked to chemical differences in formed tribofilms of LiX and PP greases, similar to what was discussed for steel surfaces in the sections above.

4.4. Grease/graphene-based additive systems are complex

The present results should not rule out graphene-based additives as friction and wear reducers in greases. However, the study has shown that the grease/graphene-based additive system is more complex and less of a universal solution than described by earlier publications [5–15, 21–24]. These typically report excellent friction and wear properties of graphene and graphene-based additives in oil and greases. In common for many of these publications are:

- i) the lack of an application and thereby a suitable evaluation method capable of simulating real contact conditions,
- ii) lack of relevant reference baselines, such as a base grease without additives or the best or standard lubricant in the intended application, and
- iii) absence of motivation behind the chosen oil and/or grease type. Further, the number of test repetitions is often not mentioned, only a few publications add error bars in friction graphs, etc., but then without describing what the error bars show. The spread of the results is often not discussed.

This study has put large effort into manufacturing greases suitable for dispersion of the additives. The positive effects of the additives in greases, with respect to friction and wear, may not be as large in a well-

working grease as if the grease in itself had inferior lubrication properties.

5. Conclusions

In the present study, greases were specifically designed to improve the dispersion of GO and rGO additives. A PAO/OSP base oil blend was used for this purpose instead of the oil blend PAO/adipate ester (in this paper called PAO oil) that has been used in earlier studies. Three additives, graphite, GO and rGO, all in a 0.1 wt% concentration, were evaluated in greases with two different thickeners, namely lithium complex (LiX) and polypropylene (PP). No positive effect from the additives could be seen, neither in the fretting tests of silver-coated copper cylinders (simulating electrical contacts) nor in the 4-ball tests of steel against steel. The PAO reference grease resulted in similar levels of friction and wear as the specially designed greases with and without additives. This indicates that optimizing the grease matrix in itself, without any additives, can be a more rewarding strategy than adding additives to a specially designed grease matrix.

A statistically significant influence from the choice of thickener was found in the 4-ball wear scar tests (steel against steel). Surfaces lubricated with PP greases showed more surface damage (both regarding wear volume and tribofilm formation) than the corresponding LiX-lubricated contacts. Two types of tribofilms formed, one containing iron and oxygen, and one based on carbon and oxygen (most likely originating from the grease constituents). The carbon signal sometimes also cohered with the iron oxide tribofilms, indicating that the grease constituents form films both on and beside iron oxide regions. Hence, the LiX and PP thickeners result in different lubricating properties for these contact conditions, where the LiX grease seems to protect the metal surfaces better. The selection of thickener type has a stronger effect on the tribological properties than the addition of graphite, GO or rGO. A better understanding of the difference in lubrication mechanisms between LiX and PP greases would require more detailed studies.

This study elucidates the complexity of graphene-based additive systems in greases. The insignificant friction and wear improvements found, demonstrates that it is far from given that graphene-based additives will improve an already well-working grease. Obviously, successful such greases are not ruled out, but would require further optimization of both the grease matrix and additive properties such as concentration, size and purity. Since the performance is strongly dependent of the tribological conditions, including parameters such as material combination, type of contact and motion, load, speed, and grease type, it is probably wise to optimize towards a selected specific application.

Credit author statement

Elin Larsson: Conceptualization, Methodology, Formal analysis, Investigation, Writing - Original Draft, Visualization, Project administration, René Westbroek: Methodology, Investigation, Resources, Writing - Review & Editing, Johan Leckner: Methodology, Resources, Writing - Review & Editing, Staffan Jacobson: Resources, Writing - Review & Editing, Supervision, Åsa Kassman Rudolphi: Conceptualization, Methodology, Resources, Writing - Review & Editing, Supervision, Funding acquisition.

Declaration of competing interest

The authors declare that they have no known competing financial interests or personal relationships that could have appeared to influence the work reported in this paper.

Acknowledgements

This work has been supported by SIO Grafen (Vinnova 2015-01467).

Leili Tahershamsi is thankfully acknowledged for the dispersion stability study of rGO in oils. The authors also thank Claire Demaille at Axel Christiernsson International AB for performing the 4-ball wear scar and seizure tests.

References

- [1] V.B. Mohan, K. Lau, D. Hui, D. Bhattacharyya, Graphene-based materials and their composites: a review on production, applications and product limitations, Compos. B Eng. 142 (2018) 200–220, <https://doi.org/10.1016/j.compositesb.2018.01.013>.
- [2] D. Berman, A. Erdemir, A.V. Suman, Graphene: a new emerging lubricant, Mater. Today 17 (2014) 31–42, <https://doi.org/10.1016/j.mattod.2013.12.003>.
- [3] A. Bianco, H.-M. Cheng, T. Enoki, Y. Gogotsi, R.H. Hurt, N. Koratkar, T. Kyotani, M. Monthoux, C.R. Park, J.M.D. Tascon, J. Zhang, All in the graphene family – A recommended nomenclature for two-dimensional carbon materials, Carbon 65 (2013) 1–6, <https://doi.org/10.1016/j.carbon.2013.08.038>.
- [4] ISO/TS 80004-13:2017 Nanotechnologies - Vocabulary - Part 13: Graphene and related two-dimensional (2D) materials, 2017.
- [5] J. Lin, L. Wang, G. Chen, Modification of graphene platelets and their tribological properties as a lubricant additive, Tribol. Lett. 41 (2011) 209–215, <https://doi.org/10.1007/s11249-010-9702-5>.
- [6] V. Eswaraiah, V. Sankaranarayanan, S. Ramaprabhu, Graphene-based engine oil nanofluids for tribological applications, ACS Appl. Mater. Interfaces 3 (2011) 4221–4227, <https://doi.org/10.1021/am200851z>.
- [7] Y. Meng, F. Su, Y. Chen, Supercritical fluid synthesis and tribological applications of silver nanoparticle-decorated graphene in engine oil nanofluid, Sci. Rep. 6 (2016), <https://doi.org/10.1038/srep31246>.
- [8] X. Fan, Y. Xia, L. Wang, W. Li, Multilayer graphene as a lubricating additive in bentone grease, Tribol. Lett. 55 (2014) 455–464, <https://doi.org/10.1007/s11249-014-0369-1>.
- [9] B.M. Kamel, A. Mohamed, M. El Sherbiny, K.A. Abed, M. Abd-Rabou, Tribological properties of graphene nanosheets as an additive in calcium grease, J. Dispersion Sci. Technol. 38 (2017) 1495–1500, <https://doi.org/10.1080/01932691.2016.1257390>.
- [10] Z.-L. Cheng, X.-X. Qin, Study on friction performance of graphene-based semi-solid grease, Chin. Chem. Lett. 25 (2014) 1305–1307, <https://doi.org/10.1016/j.clet.2014.03.010>.
- [11] J. Wang, X. Guo, Y. He, M. Jiang, K. Gu, Tribological characteristics of graphene as grease additive under different contact forms, Tribol. Int. 127 (2018) 457–469, <https://doi.org/10.1016/j.triboint.2018.06.026>.
- [12] T. Ouyang, Y. Shen, R. Yang, L. Liang, H. Liang, B. Lin, Z.Q. Tian, P.K. Shen, 3D hierarchical porous graphene nanosheets as an efficient grease additive to reduce wear and friction under heavy-load conditions, Tribol. Int. 144 (2020), 106118, <https://doi.org/10.1016/j.triboint.2019.106118>.
- [13] H. Fu, G. Yan, M. Li, H. Wang, Y. Chen, C. Yan, C.-T. Lin, N. Jiang, J. Yu, Graphene as a nanofiller for enhancing the tribological properties and thermal conductivity of base grease, RSC Adv. 9 (2019) 42481–42488, <https://doi.org/10.1039/C9RA09201C>.
- [14] Z. Li, Q. He, S. Du, Y. Zhang, Effect of few layer graphene additive on the tribological properties of lithium grease, Lubric. Sci. 32 (2020) 333–343, <https://doi.org/10.1002/lsc.1506>.
- [15] A. Mohamed, V. Tirth, B.M. Kamel, Tribological characterization and rheology of hybrid calcium grease with graphene nanosheets and multi-walled carbon nanotubes as additives, J. Mater. Res. Technol. 9 (2020) 6178–6185, <https://doi.org/10.1016/j.jmrt.2020.04.020>.
- [16] F. Mao, U. Wiklund, A.M. Andersson, U. Jansson, Graphene as a lubricant on Ag for electrical contact applications, J. Mater. Sci. 50 (2015) 6518–6525, <https://doi.org/10.1007/s10853-015-9212-9>.
- [17] D. Berman, A. Erdemir, A.V. Suman, Graphene as a protective coating and superior lubricant for electrical contacts, Appl. Phys. Lett. 105 (2014), 231907, <https://doi.org/10.1063/1.4903933>.
- [18] D. Berman, A. Erdemir, A.V. Suman, Few layer graphene to reduce wear and friction on sliding steel surfaces, Carbon 54 (2013) 454–459, <https://doi.org/10.1016/j.carbon.2012.11.061>.
- [19] D. Berman, A. Erdemir, A.V. Suman, Reduced wear and friction enabled by graphene layers on sliding steel surfaces in dry nitrogen, Carbon 59 (2013) 167–175, <https://doi.org/10.1016/j.carbon.2013.03.006>.
- [20] M.-S. Won, O.V. Penkov, D.-E. Kim, Durability and degradation mechanism of graphene coatings deposited on Cu substrates under dry contact sliding, Carbon 54 (2013) 472–481, <https://doi.org/10.1016/j.carbon.2012.12.007>.
- [21] Z. Chen, Y. Liu, J. Luo, Tribological properties of few-layer graphene oxide sheets as oil-based lubricant additives, Chin. J. Mech. Eng. 29 (2016) 439–444, <https://doi.org/10.3901/CJME.2015.1028.129>.
- [22] H. Song, Z. Wang, J. Yang, Tribological properties of graphene oxide and carbon spheres as lubricating additives, Appl. Phys. A 122 (2016), <https://doi.org/10.1007/s00339-016-0469-x>.
- [23] H.P. Mungse, O.P. Khatri, Chemically functionalized reduced graphene oxide as a novel material for reduction of friction and wear, J. Phys. Chem. C 118 (2014) 14394–14402, <https://doi.org/10.1021/jp5033614>.
- [24] J. Singh, G. Anand, D. Kumar, N. Tandon, Graphene based composite grease for elastohydrodynamic lubricated point contact, IOP Conf. Ser. Mater. Sci. Eng. 149 (2016), 012195, <https://doi.org/10.1088/1757-899X/149/1/012195>.

- [25] H. Liang, Y. Bu, J. Zhang, Z. Cao, A. Liang, Graphene oxide film as solid lubricant, *ACS Appl. Mater. Interfaces* 5 (2013) 6369–6375, <https://doi.org/10.1021/am401495y>.
- [26] F. Andersson, *Graphene and Graphene Oxide as New Lubricants in Industrial Applications*, Master Thesis, Uppsala University, 2015.
- [27] In Nanotechnologies – Vocabulary – Part 13: Graphene and Related Two-Dimensional (2D) Materials, International Organization for Standardization (ISO), 2017.
- [28] O. Penkov, Introduction to graphene, in: *Tribology of Graphene: Simulation Methods, Preparation Methods, and Their Applications*, Elsevier, Waltham, 2020, pp. 1–10.
- [29] V.B. Mohan, K. Jayaraman, M. Stamm, D. Bhattacharyya, Physical and chemical mechanisms affecting electrical conductivity in reduced graphene oxide films, *Thin Solid Films* 616 (2016) 172–182, <https://doi.org/10.1016/j.tsf.2016.08.007>.
- [30] A.P. Kauling, A.T. Seefeldt, D.P. Pisoni, R.C. Pradeep, R. Bentini, R.V.B. Oliveira, K. S. Novoselov, A.H. Castro Neto, The worldwide graphene flake production, *Adv. Mater.* (2018), 1803784, <https://doi.org/10.1002/adma.201803784>.
- [31] ISO/TS 21356-1:2021 Nanotechnologies - Structural characterization of graphene - Part 1: Graphene from powders and dispersions, 2021.
- [32] H.D. Huang, J.P. Tu, L.P. Gan, C.Z. Li, An investigation on tribological properties of graphite nanosheets as oil additive, *Wear* 261 (2006) 140–144, <https://doi.org/10.1016/j.wear.2005.09.010>.
- [33] D.W. Johnson, B.P. Dobson, K.S. Coleman, A manufacturing perspective on graphene dispersions, *Curr. Opin. Colloid Interface Sci.* 20 (2015) 367–382, <https://doi.org/10.1016/j.cocis.2015.11.004>.
- [34] G. Gow, Lubricating grease, in: *Chemistry and Technology of Lubricants*, third ed., Springer, 2010.
- [35] B. Jacobson, *Polymer Thickened Lubricant*, White paper Lubrisense, Axel Christiernsson AB, 2007.
- [36] L.A.T. Honary, E.W. Richter, *Biobased Lubricants and Greases: Technology, and Products*, Wiley, Hoboken, N.J, 2011.
- [37] J. Leckner, Energy efficiency and lubrication mechanisms of polymer thickened greases, in: 27th ELGI Annual General Meeting, Barcelona, Spain, 2015.
- [38] J. Leckner, R. Westbroek, Polypropylene - a new thickener technology for energy efficient lubrication, in: NLGI 83rd Annual Meeting, Hot Springs, VA, USA, 2016.
- [39] E. Larsson, A.M. Andersson, Å. Kassman Rudolph, Grease lubricated fretting of silver coated copper electrical contacts, *Wear* 376–377 (2017) 634–642, <https://doi.org/10.1016/j.wear.2017.02.022>.
- [40] J. Shu, K. Harris, B. Munavirov, R. Westbroek, J. Leckner, S. Glavatskikh, Tribology of polypropylene and Li-complex greases with ZDDP and MoDTC additives, *Tribol. Int.* 118 (2018) 189–195, <https://doi.org/10.1016/j.triboint.2017.09.028>.
- [41] M. Greaves, Oil soluble synthetic polyalkylene glycols A new type of group V base oil, *Lube Magazine* 104 (2011) 21–24.
- [42] D. Konios, M.M. Stylianakis, E. Stratakis, E. Kymakis, Dispersion behaviour of graphene oxide and reduced graphene oxide, *J. Colloid Interface Sci.* 430 (2014) 108–112, <https://doi.org/10.1016/j.jcis.2014.05.033>.
- [43] C. Roman, C. Valencia, J.M. Franco, AFM and SEM assessment of lubricating grease microstructures: influence of sample preparation protocol, frictional working conditions and composition, *Tribol. Lett.* 63 (2016) 20, <https://doi.org/10.1007/s11249-016-0710-y>.
- [44] N. De Laurentis, P. Cann, P.M. Lugt, A. Kadircic, The influence of base oil properties on the friction behaviour of lithium greases in rolling/sliding concentrated contacts, *Tribol. Lett.* 65 (2017), <https://doi.org/10.1007/s11249-017-0908-7>.
- [45] F. Cyriac, P.M. Lugt, R. Bosman, C.J. Padberg, C.H. Venner, Effect of thickener particle geometry and concentration on the grease EHL film thickness at medium speeds, *Tribol. Lett.* 61 (2016) 1–13, <https://doi.org/10.1007/s11249-015-0633-z>.
- [46] D. Muller, C. Matta, R. Thijssen, M.N. bin Yusof, M.C.P. van Eijk, S. Chatra, Novel polymer grease microstructure and its proposed lubrication mechanism in rolling/sliding contacts, *Tribol. Int.* 110 (2017) 278–290, <https://doi.org/10.1016/j.triboint.2017.02.030>.
- [47] DIN 51350-1:2015-03, *Testing of Lubricants - Testing in the Four-Ball Tester - Part 1: General Working Principles*, 2015.
- [48] W.J. Bartz, Solid lubricant additives—effect of concentration and other additives on anti-wear performance, *Wear* 17 (1971) 421–432, [https://doi.org/10.1016/0043-1648\(71\)90048-2](https://doi.org/10.1016/0043-1648(71)90048-2).
- [49] W. Zhang, M. Zhou, H. Zhu, Y. Tian, K. Wang, J. Wei, F. Ji, X. Li, Z. Li, P. Zhang, D. Wu, Tribological properties of oleic acid-modified graphene as lubricant oil additives, *J. Phys. Appl. Phys.* 44 (2011), 205303, <https://doi.org/10.1088/0022-3727/44/20/205303>.
- [50] A. Neyman, J. Sikora, Grease effect on fretting wear of mild steel, *Ind. Lubric. Tribol.* 60 (2008) 67–78, <https://doi.org/10.1108/00368790810858368>.
- [51] J. Leckner, R. Westbroek, Polypropylene - a novel thickener technology with many surprises, in: 29th ELGI AGM, Finland, Helsinki, 2017.
- [52] ASTM D7152-11(2016)e1. Standard Practice for Calculating Viscosity of a Blend of Petroleum Products, ASTM International, West Conshohocken, PA, 2016.
- [53] L.W. Budd Lee, Comparing conventional PAGs to oil soluble polyalkylene glycols, in: Society of Tribologists and Lubrication Engineers 68th Annual Meeting & Exhibition, 2013. Detroit, USA.
- [54] N. De Laurentis, A. Kadircic, P. Lugt, P. Cann, The influence of bearing grease composition on friction in rolling/sliding concentrated contacts, *Tribol. Int.* 94 (2016) 624–632, <https://doi.org/10.1016/j.triboint.2015.10.012>.
- [55] Y. Kimura, T. Endo, D. Dong, EHL with Grease at Low Speeds, in: *Advanced Tribology*, Springer, Berlin, Heidelberg, 2010, pp. 15–19.
- [56] H. Kimura, Y. Imai, Y. Yamamoto, Study on fiber length control for ester-based lithium soap grease, *Tribol. Trans.* 44 (2001) 405–410, <https://doi.org/10.1080/10402000108982474>.
- [57] M.A. Delgado, C. Valencia, M.C. Sánchez, J.M. Franco, C. Gallegos, Influence of soap concentration and oil viscosity on the rheology and microstructure of lubricating greases, *Ind. Eng. Chem. Res.* 45 (2006) 1902–1910, <https://doi.org/10.1021/ie050826f>.
- [58] J.F. Moulder, W.F. Stickle, P.E. Sobol, K.D. Bomben, J. Chastain, R.C. King Jr., *Physical electronics, incorporation*, in: *Handbook of X-Ray Photoelectron Spectroscopy: a Reference Book of Standard Spectra for Identification and Interpretation of XPS Data*, Physical Electronics, Eden Prairie, Minn., 1995.